



Defense Threat Reduction Agency  
8725 John J. Kingman Road, MS-6201  
Fort Belvoir, VA 22060-6201



DTRA-TR-15-9

# TECHNICAL REPORT

## Glasses for Detection of Penetrating Radiation via the Cherenkov Effect

Distribution Statement A. Approved for public release;  
distribution is unlimited.

July 2015

HDTRA1-09-1-0052

Jason P. Hayward

Prepared by:  
University of Tennessee  
201 Andy Holt Tower  
Knoxville, TN 37996

**DESTRUCTION NOTICE:**

Destroy this report when it is no longer needed.  
Do not return to sender.

PLEASE NOTIFY THE DEFENSE THREAT REDUCTION  
AGENCY, ATTN: DTRIAC/ J9STT, 8725 JOHN J. KINGMAN ROAD,  
MS-6201, FT BELVOIR, VA 22060-6201, IF YOUR ADDRESS  
IS INCORRECT, IF YOU WISH THAT IT BE DELETED FROM THE  
DISTRIBUTION LIST, OR IF THE ADDRESSEE IS NO  
LONGER EMPLOYED BY YOUR ORGANIZATION.

<b>REPORT DOCUMENTATION PAGE</b>				<i>Form Approved</i> <b>OMB No. 0704-0188</b>	
Public reporting burden for this collection of information is estimated to average 1 hour per response, including the time for reviewing instructions, searching existing data sources, gathering and maintaining the data needed, and completing and reviewing this collection of information. Send comments regarding this burden estimate or any other aspect of this collection of information, including suggestions for reducing this burden to Department of Defense, Washington Headquarters Services, Directorate for Information Operations and Reports (0704-0188), 1215 Jefferson Davis Highway, Suite 1204, Arlington, VA 22202-4302. Respondents should be aware that notwithstanding any other provision of law, no person shall be subject to any penalty for failing to comply with a collection of information if it does not display a currently valid OMB control number. <b>PLEASE DO NOT RETURN YOUR FORM TO THE ABOVE ADDRESS.</b>					
<b>1. REPORT DATE (DD-MM-YYYY)</b> 00-07-2015		<b>2. REPORT TYPE</b> Technical		<b>3. DATES COVERED (From - To)</b> August 17, 2009 - August 16, 2014	
<b>4. TITLE AND SUBTITLE</b> Glasses for Detection of Penetrating Radiation via the Cherenkov Effect				<b>5a. CONTRACT NUMBER</b> HDTRA1-09-1-0052	
				<b>5b. GRANT NUMBER</b>	
				<b>5c. PROGRAM ELEMENT NUMBER</b>	
<b>6. AUTHOR(S)</b> Jason P. Hayward				<b>5d. PROJECT NUMBER</b> R011382194	
				<b>5e. TASK NUMBER</b>	
				<b>5f. WORK UNIT NUMBER</b>	
<b>7. PERFORMING ORGANIZATION NAME(S) AND ADDRESS(ES)</b> University of Tennessee 201 Andy Holt Tower Knoxville, TN 37996				<b>8. PERFORMING ORGANIZATION REPORT NUMBER</b>	
<b>9. SPONSORING / MONITORING AGENCY NAME(S) AND ADDRESS(ES)</b> Defense Threat Reduction Agency 8725 John J. Kingman Road STOP 6201 Fort Belvoir, VA 22060				<b>10. SPONSOR/MONITOR'S ACRONYM(S)</b> DTRA	
				<b>11. SPONSOR/MONITOR'S REPORT NUMBER(S)</b> DTRA-TR-15-9	
<b>12. DISTRIBUTION / AVAILABILITY STATEMENT</b> Approved for public release; distribution is unlimited.					
<b>13. SUPPLEMENTARY NOTES</b>					
<b>14. ABSTRACT</b> In this research, we investigated the properties of glasses suitable for detection of ionizing radiation (i.e., MeV gammas) via the Cherenkov effect. We established the materials properties and learned the fabrication techniques of materials suitable for the production of Cherenkov light, but with an investigative approach that is tailored and specialized to support photofission and muonic x-ray detection for counter-WMD application. The response of the glasses was also investigated so that sensitivity and specificity of standoff detection systems based upon our efforts may be understood.					
<b>15. SUBJECT TERMS</b> Cherenkov   Photofission   Isotopic   Gammas   Photosensor					
<b>16. SECURITY CLASSIFICATION OF:</b>			<b>17. LIMITATION OF ABSTRACT</b>  SAR	<b>18. NUMBER OF PAGES</b>  27	<b>19a. NAME OF RESPONSIBLE PERSON</b> David Petersen
<b>a. REPORT</b> Unclassified	<b>b. ABSTRACT</b> Unclassified	<b>c. THIS PAGE</b> Unclassified			<b>19b. TELEPHONE NUMBER (include area code)</b> 703-767-3164

# CONVERSION TABLE

Conversion Factors for U.S. Customary to metric (SI) units of measurement.

MULTIPLY → BY → TO GET  
TO GET ← BY ← DIVIDE

angstrom	1.000 000 x E -10	meters (m)
atmosphere (normal)	1.013 25 x E +2	kilo pascal (kPa)
bar	1.000 000 x E +2	kilo pascal (kPa)
barn	1.000 000 x E -28	meter <sup>2</sup> (m <sup>2</sup> )
British thermal unit (thermochemical)	1.054 350 x E +3	joule (J)
calorie (thermochemical)	4.184 000	joule (J)
cal (thermochemical/cm <sup>2</sup> )	4.184 000 x E -2	mega joule/m <sup>2</sup> (MJ/m <sup>2</sup> )
curie	3.700 000 x E +1	*giga bacquerel (GBq)
degree (angle)	1.745 329 x E -2	radian (rad)
degree Fahrenheit	$t_k = (t^{\circ}f + 459.67) / 1.8$	degree kelvin (K)
electron volt	1.602 19 x E -19	joule (J)
erg	1.000 000 x E -7	joule (J)
erg/second	1.000 000 x E -7	watt (W)
foot	3.048 000 x E -1	meter (m)
foot-pound-force	1.355 818	joule (J)
gallon (U.S. liquid)	3.785 412 x E -3	meter <sup>3</sup> (m <sup>3</sup> )
inch	2.540 000 x E -2	meter (m)
jerk	1.000 000 x E +9	joule (J)
joule/kilogram (J/kg) radiation dose absorbed	1.000 000	Gray (Gy)
kilotons	4.183	terajoules
kip (1000 lbf)	4.448 222 x E +3	newton (N)
kip/inch <sup>2</sup> (ksi)	6.894 757 x E +3	kilo pascal (kPa)
ktap	1.000 000 x E +2	newton-second/m <sup>2</sup> (N-s/m <sup>2</sup> )
micron	1.000 000 x E -6	meter (m)
mil	2.540 000 x E -5	meter (m)
mile (international)	1.609 344 x E +3	meter (m)
ounce	2.834 952 x E -2	kilogram (kg)
pound-force (lbs avoirdupois)	4.448 222	newton (N)
pound-force inch	1.129 848 x E -1	newton-meter (N-m)
pound-force/inch	1.751 268 x E +2	newton/meter (N/m)
pound-force/foot <sup>2</sup>	4.788 026 x E -2	kilo pascal (kPa)
pound-force/inch <sup>2</sup> (psi)	6.894 757	kilo pascal (kPa)
pound-mass (lbm avoirdupois)	4.535 924 x E -1	kilogram (kg)
pound-mass-foot <sup>2</sup> (moment of inertia)	4.214 011 x E -2	kilogram-meter <sup>2</sup> (kg-m <sup>2</sup> )
pound-mass/foot <sup>3</sup>	1.601 846 x E +1	kilogram-meter <sup>3</sup> (kg/m <sup>3</sup> )
rad (radiation dose absorbed)	1.000 000 x E -2	**Gray (Gy)
roentgen	2.579 760 x E -4	coulomb/kilogram (C/kg)
shake	1.000 000 x E -8	second (s)
slug	1.459 390 x E +1	kilogram (kg)
torr (mm Hg, 0° C)	1.333 22 x E -1	kilo pascal (kPa)

\*The bacquerel (Bq) is the SI unit of radioactivity; 1 Bq = 1 event/s.

\*\*The Gray (GY) is the SI unit of absorbed radiation.

**Grant/Award #: HDTRA1-09-1-0052**

**PI Name: Jason Hayward**

**Organization/Institution: The University of Tennessee**

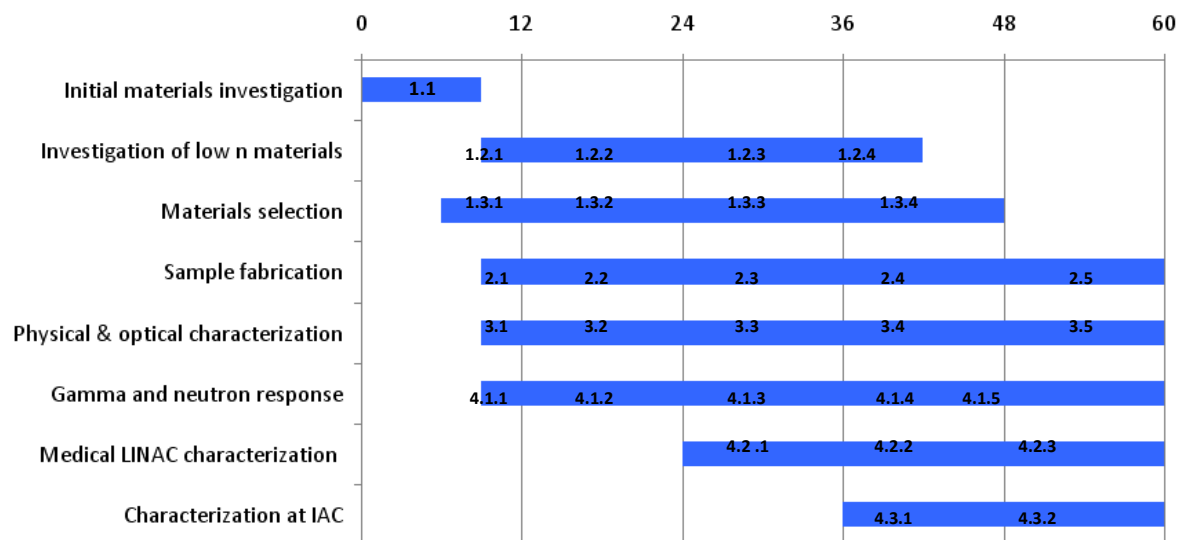
**Project Title: Glasses for detection of penetrating radiation via the Cherenkov effect**

**What are the major goals of the project?**

*List the major goals of the project as stated in the approved application or as approved by the agency. If the application lists milestones/target dates for important activities or phases of the project, identify these dates and show actual completion dates or the percentage of completion. Generally, the goals will not change from one reporting period to the next. However, if the awarding agency approved changes to the goals during the reporting period, list the revised goals and objectives. Also explain any significant changes in approach or methods from the agency approved application or plan.*

In this research, we investigated the properties of glasses suitable for detection of ionizing radiation (i.e., MeV gammas) via the Cherenkov effect. We established the materials properties and learned the fabrication techniques of materials suitable for the production of Cherenkov light, but with an investigative approach that is tailored and specialized to support photofission and muonic x-ray detection for counter-WMD application. The response of the glasses was also investigated so that sensitivity and specificity of standoff detection systems based upon our efforts may be understood.

**Project schedule**



At the end of 60 months of project funding, all tasks have been completed.

**What was accomplished under these goals?**

*For this reporting period describe: 1) major activities; 2) specific objectives; 3) significant results, including major findings, developments, or conclusions (both positive and negative); and 4) key outcomes or other achievements. Include a discussion of stated goals not met. As the project progresses, the emphasis in reporting in this section should shift from reporting activities to reporting accomplishments.*

Progress toward achieving our research objectives as specified in our statement of work is complete, and some directions have been taken beyond the SOW (e.g., simulation and modeling work, measurements to understand active in DT generator tagged interrogation of DU) to better understand application to DTRA detection priorities.

In the first three years of the program (while our annual budget was the largest), we worked with Oak Ridge National Laboratory to fabricate 123 glass samples. Several families of glass formers were investigated, and some large samples were fabricated. We performed optical and physical characterization of these samples. Most of them were optically transparent, non-hygroscopic, and durable for handling and mounting to a photosensor. We also characterized the samples with isotopic sources in order to understand their response to gammas and neutrons. Three peer-reviewed publications were written about this work, each of them published in 2013. This year, in work that we are nearly done preparing for publication, we compared measurements of fission gammas in same-size glasses to determine the desirable material properties of glasses. We found that both low optical absorption edge and high density are necessary in order to yield the highest detection efficiency for counting Cf-252 fission gammas. It is important for the dense glass to have a low optical absorption edge so that enough optical photons are generated and collected to, in turn, generate enough photoelectrons (above the electronic threshold) in the photosensor so that a count is registered. The glasses that we fabricated in this program are still less efficient for fission gammas than the PbF<sub>2</sub> single crystal (7.77 g/cm<sup>3</sup>, absorption edge of 290 nm) that represented our standard of comparison in that study because we did not make any glasses that exceeded 6 g/cm<sup>3</sup>, and our optical absorption edge tended to increase along with the increases in density afforded by loading compounds like PbO and bismuth compounds. In our materials discovery program, our lowest absorption absorption edges (<250 nm) were achieved for glasses with densities < 3.5 g/cm<sup>3</sup>. Thus, it remains to be seen whether Cherenkov glasses are capable of exceeding the detection performance of single crystal PbF<sub>2</sub> when one considers fission gamma sensing. In any case, Cherenkov glasses are much more dense than plastic scintillators (~1 g/cm<sup>3</sup>), so they should certainly exceed their efficiency for sensing fission gamma rays.

During the course of the project, we made three measurement campaigns at the Idaho Accelerator Center (IAC) to characterize Cherenkov glass samples with LINAC beams from 6-40 MeV (using pulse widths as short as 50 ps), to understand Cherenkov glass detector sensing capabilities in the prompt regime, and to understand sources of active background—also in the prompt regime—in said measurements. Two peer-reviewed publications came out in 2014 about this work, and one more regarding our moderate to high Z ‘gamma LIDAR’ investigation is under review. Beyond the IAC measurements, we also added to the SOW by including tagged DT interrogation measurements in an effort to understand the prompt response and active background observed in this case. In order to understand our interrogation measurements (short pulse x-ray Linac and DT), we have used detailed MCNP simulations of the accelerator, targets, and detector assembly. Modeling and data analysis of experiments at the IAC is complete. By comparing simulations and measurements we have a good understanding of the mix of prompt fission gammas and prompt active background radiations that we are observing in coincidence with the prompt flash striking a target of depleted uranium (fissionable, high Z) or lead (non-fissionable, high Z). In particular, the prompt active background coincident with

prompt gammas contains a substantial flux of 1) annihilation radiation from pair production in the target, 2) secondary bremsstrahlung radiation from the charged particles produced by all photo-interactions in the target, and 3) Rayleigh scattering of energetic gammas including gammas produced from 1 and 2. While the intrinsic Cherenkov threshold may discriminate against detection of individual 511 keV gammas rather well because they tend to produce very few photons when they do interact, note that the annihilation radiation yield from any photo-induced 'radiation flash' in a high Z target produces many annihilation gammas that may hit a single detector in coincidence. A thin filter (e.g., 15 mm of Pb) in front of the Cherenkov glass sensor helps to reduce this large 511 keV flux. Yet, even when strict timing cuts and energy thresholds<sup>1</sup> are employed, any method to sense prompt fission gammas induced by photofission in Cherenkov glass detectors must rely on the ability to detect statistically larger quantities of Cherenkov light, observed, for example as integrated charge per pulse in a PMT, above what would be produced by the prompt active background due to a particular target. Results from our MCNP simulations suggest that the fraction of prompt fission gammas sensed per prompt active background gamma is less than 1 in 10 after timing and energy cuts. This study is documented in our peer-reviewed paper called "Investigation of active background from photofission in depleted uranium using Cherenkov detectors and gamma ray time-of-flight analysis." Although the prompt fission gammas from photofission cannot be sensed due to the more intense gamma background, perhaps our ongoing analysis with the tagged DT source will suggest that the case is different in neutron interrogation.

This project has educated 7 University of Tennessee graduate students (1 full time), 7 undergraduate students, and 3 postdocs who have participated in research. Six graduate students supported at least in part by this project completed their M.S. degrees in Nuclear Engineering. Five students who have received some support from this project are still pursuing Ph.D. degrees. Knowledge from research outcomes has been integrated into University of Tennessee nuclear security science graduate coursework in one course, as described below.

Additionally, five invention disclosures related to this project work were submitted to the University of Tennessee; unfortunately, since the government was expected to be the main customer for each area, the University chosen to pursue none of them for patenting.

Next, the significant results from each of our peer-reviewed publications, in order, are listed below. After that, the significant results from papers under review or in preparation are listed.

1) J.P. Hayward, Z.W. Bell, L.A. Boatner, C.L. Hobbs, R.E. Johnson, J.O. Ramey, G.E. Jellsion, Jr., "Characterizing the response of Cherenkov glass detectors with isotopic gamma-ray sources," *Journal of Radioanalytical and Nuclear Chemistry*, Feb. 2013, Vol. 295, Issue 2, pp. 1143-1151.

In this paper, counting measurements of low-energy gammas incident from isotopic sources upon representative Cherenkov glass detectors were reported. The glass samples, only 7–15 mm thick, have a low efficiency for gamma ray detection. Efficiency for high-energy photons was found to be mainly affected by traditional attributes such as density,  $Z_{\text{eff}}$ , and size. Absolute counting measurements of low energy gamma-ray sources with Cherenkov glass detectors having a PMT readout were found to be complicated by the bias-dependent response of the PMT both to radiation background and the isotopic

---

<sup>1</sup> When energy thresholds and cuts are mention, gamma spectroscopy in the conventional sense is not implied. Rather, lower (and upper) level gating based upon the recorded number of photoelectrons, as determined by integrated charge/pulse in a calibrated photosensor, is implied.

source being measured. Since the distributions of photoelectron observables tend to peak at the single photoelectron level, light collection efficiency considerations affect the absolute count rate when measuring low energy photons from isotopic sources. In the presence of an isotopic source, a net response was determined by making a counting measurement, then subtracting a measurement using the same setup, where the Cherenkov light produced from the glass sample was blocked. The pulse height response from gamma ray interactions was found to be not very well separated from the noise and background, but separation was found to improve for higher energy gamma sources which tend to deposit more energy, producing more Cherenkov light per event. A difference in pulse height response (compared to gamma background) was observed in measurements of a moderated PuBe source. Improved light collection efficiency is also expected to produce a shift in the pulse height distribution, moving the measured distribution away from one photoelectron. An analysis of the simulation results was used to facilitate the interpretation of measured results. This work discussed the behavior of monolithic Cherenkov glass detectors in the context of their use with isotopic gamma-ray sources. Although thin Cherenkov glass detectors with conventional PMT readout are not useful for high efficiency detection of low-energy gamma-rays because the signal is buried in the dark noise, this characterization sets the groundwork to evaluate large Cherenkov glass detector systems for sensitivity to MeV photons and specificity against passive or active backgrounds, i.e., radiation backgrounds where an interrogating source is absent or present, respectively.

2) J.P. Hayward, Z.W. Bell, L.A. Boatner, C.L. Hobbs, R.E. Johnson, J.O. Ramey, G.E. Jellison, Jr., "Simulated Response of Cherenkov Glass Detectors to MeV Photons," *Journal of Radioanalytical and Nuclear Chemistry*, Feb. 2013, Vol. 295, Issue 2, pp. 1321-1329.

Non-scintillating glasses are expected to be capable of detecting MeV photons at high event rates with a time response of  $\sim 100$  ps. High efficiency detection of MeV photons requires large glass volumes that are several cm thick. Selective detection of MeV photons requires that the photoelectron yield is maximized so that a threshold can be applied to discriminate against background radiations. High photoelectron yield also allows one to deduce the deposited energy. The energy of incident gamma rays can be best inferred in the case that the detector's volume is sufficiently large so that any interaction in the glass sample is very likely to result in full energy deposition. Simulations of single glass layers suggest that the mean number of photoelectrons will remain high when layers of thickness 1-3 cm are stacked, resulting in lower photon loss compared to very thick single layers. The photoelectron yield is improved through use of glasses with high transparency in the UV and photosensors with a matching spectral response. Reflecting the glass detector is important for improved photoelectron production in layered detectors, but it degrades timing performance. The efficiency of glass Cherenkov detectors for MeV photons from SNM can potentially be greater than for use of plastic scintillators or water Cherenkov detectors, based upon the fact that density and  $Z_{\text{eff}}$  can be substantially higher in glasses compared with plastic or water.

3) B. Ayaz-Maierhafer, J.P. Hayward, Z.W. Bell, L.A. Boatner, R.E. Johnson, "Measurements of thermal neutron response in Cherenkov glass designed for MeV photon detection," *IEEE Transactions on Nuclear Science*, Vol. 60, Issue 2, May 2013, p. 701-707.

In this paper, the neutron response of selected, optically clear Cherenkov glasses was investigated via time-dependent counting measurements and high-resolution gamma spectroscopy of beta and/or gamma activation products. Glasses that respond well to neutron activation could be used in place of activation foils. Glasses designed for specificity to MeV photon detection should ideally not respond to neutron irradiation. This research suggests that glass constituents with low thermal neutron capture



probabilities, containing isotopes with low abundances, producing long half-life activation products with low gamma and beta energies are good candidates to use when attempting to minimize the response to thermal neutrons. A lithium lead phosphate glass and a calcium lead phosphate glass reported in this paper was the least responsive to neutron irradiation.

4) X. Zhang, J.P. Hayward, M.A. Laubach, "New method to remove the electronic noise for absolutely calibrating low gain photomultiplier tube with a higher precision," *Nuclear Instruments and Methods in Physics Research A*, Vol. 755, Aug. 2014, p. 32-37.

A new method based on the fall time difference between the electronic noise and the real signal for the calibration of PMT single photon response is proposed and validated with experiments. With this method, the electronic noise and the real signals can be separated, except for a few percent of very small signals heavily influenced by the electronic noise. Using a convolution based on an integral transform, even these small signals can also be separated very well. This method allows us to calibrate low gain PMTs without the interference of electronic noise, so higher precision can be expected. One application that this method allows is for us to explore the energy relationship for gamma sensing in Cherenkov radiators while maintaining the fastest possible time-of-flight response in 51-mm PMTs (i.e., with the H10570 PMT) and high dynamic range.

5) B. Ayaz-Maierhafer, X. Zhang, J.P. Hayward, Z.W. Bell, M.A. Laubach "Investigation of active background from photofission in depleted uranium using Cherenkov detectors and gamma ray time-of-flight analysis," *IEEE Transactions on Nuclear Science*, Vol. 61, No. 4, Aug. 2014, p. 2402-2409

Prompt gammas from induced fission ( $\sim 7/\text{fission}$ ) could potentially be a valuable fission signature to use for detection of SNM like HEU. Detectability requires an understanding of both signal and background, and the background from dense, high Z SNM like HEU has been investigated in this work by using DU as a surrogate. In order to study the prompt gamma signature and associated active backgrounds from SNM induced through photofission, especially in the context of standoff detection, a combination of measurements using the IAC 44 MeV LINAC and MCNPX simulations were used. In particular, we showed the prompt, time-gated glass Cherenkov detector response to gamma emissions resulting from short pulse 6, 10, and 25 MeV bremsstrahlung beams incident on a DU target. The fast time response of the system (CRT of 93 ps FWHM) allowed prompt emissions from the target to be selected for analysis using gamma ray time-of-flight. As the beam energy increases, the combination of active background and fission gamma rays observed from each flash on the target by the Cherenkov glass detector become more significant. Additionally, a relationship between beam energy, energy deposition, and the recorded photoelectron frequency distributions in Cherenkov glass detectors was observed. In order of prominence, MCNPX simulations showed that secondary bremsstrahlung, annihilation, Compton scattering, and coherent scattering are all significant contributors to the background that is coincident with prompt gammas. Furthermore, the high likelihood of multiple photon interactions occurring in the target increases the background observed at a back angle. Increasing the Cherenkov detector threshold is expected to reduce the contribution from annihilation gammas. However, considering any threshold used with the Cherenkov detectors, the prompt fission gamma signal from depleted uranium is buried in the active background from the interrogating photon source. From these results, it appears that the time-gated Cherenkov detector measurements described here are not appropriate for sensitive detection of a prompt fission gamma signal in a depleted uranium target. On the other hand, one may expect that the active background may have some specificity to the target material and geometry.

6) X. Zhang, B. Ayaz-Maierhafer, M.A. Laubach, J.P. Hayward, "Observation of Material, Thickness, and Bremsstrahlung X-ray Intensity Dependent Effects in Moderate and High Z Targets in a Gamma Ray LIDAR Experiment," submitted to *Nuclear Instruments and Methods in Physics Research A*, July 2014, under review.

The response of a gamma ray LIDAR system to different moderate and high Z target materials and thicknesses was investigated. The system consisted of a fast pulse (~50 ps) LINAC and a Cherenkov detector. The sub-100 ps timing resolution allowed the system to achieve 3 cm depth resolving ability. The long lifetime of positrons produced through the annihilation process in targets, such as 110 ps in iron and 194 ps in lead, worsen the depth resolving ability of the detection system. Thus, a higher threshold is desirable to mitigate this influence. Because the intrinsic energy threshold of the Cherenkov detector is 340.7 keV, low energy Compton scattering gammas in the experimental reference frame are not registered by the detector. Thus, only annihilation and high energy secondary bremsstrahlung gammas with a  $Z^2$  or higher order dependence are recorded by the detector, which increases the system material or Z resolving capability compared with detection systems which are sensitive to Compton scattering gammas, which depend on Z. Due to this advantage, a factor of five of gamma yield difference between iron targets and DU/lead targets has been observed for 20 MeV bremsstrahlung X-rays. In addition, experiments show that iron targets tend to produce less energetic gammas compared with lead and DU targets. Combining this with the gamma yields of targets, a better material resolving capability should be obtained. Furthermore, due to the self-shielding effect, simulations with MCNPX show that lead targets produce more gammas than DU targets when the target thicknesses are larger than 15 mm and 20 mm for 20 or 40 MeV bremsstrahlung X-rays, respectively. Experimental results for one-inch thick lead and DU targets at 20 MeV show consistency with simulation results. The experimental results with various charge per pulse in the range of 1 to 2.5 nC can yield a better separation between lead and DU targets in the same situation. Thus, in a given system, an optimized bremsstrahlung X-ray intensity is necessary to achieve the best resolving capability of materials (and their Zs). In summary, a suitable energy threshold of Cherenkov detectors and an optimal bremsstrahlung X-ray intensity are important.

7) B. Ayaz-Maierhafer, M.A. Laubach, J.P. Hayward, "Sensing of Cf-252 Fission Gamma Rays Using Same-Size Glass Detectors," being prepared for submission to NIM A.

The objective of this experimental work was to investigate the capabilities of same-size glass Cherenkov detectors to sense  $^{252}\text{Cf}$  fission gammas through time-of-flight analysis. When it comes to fission gamma ray sensing, it is not straightforward how to determine the detection efficiency for Cherenkov glasses because it depends strongly on light collection efficiency. Eight same-size Cherenkov detectors were tested, including 7 glasses and one crystal, all of which were purchased from commercial sources. They were chosen to vary in density, refractive index and optical absorption. We studied the effects of absorption edge, density, and threshold energy on several same-size Cherenkov detectors to sense the fission gammas. From these results, it can be concluded that the Cherenkov glasses should be dense and have a low optical absorption edge to sense fission gammas most efficiently. This is consistent with what has been observed for Cherenkov radiators used in high-energy physics to sense various types of electromagnetic radiation.

**What opportunities for training and professional development has the project provided?**

*If the research is not intended to provide training and professional development opportunities or there is nothing significant to report during this reporting period, state “Nothing to Report.” Describe opportunities for training and professional development provided to anyone who worked on the project or anyone who was involved in the activities supported by the project. “Training” activities are those in which individuals with advanced professional skills and experience assist others in attaining greater proficiency. Training activities may include, for example, courses or one-on-one work with a mentor. “Professional development” activities result in increased knowledge or skill in one’s area of expertise and may include workshops, conferences, seminars, study groups, and individual study. Include participation in conferences, workshops, and seminars not listed under major activities.*

During the five years of support, the project that helped to support the project participants in attending conferences—and sometimes short courses at conferences—and presenting at conferences including the IEEE Nuclear Science Symposia in Orlando, Knoxville, Spain, and South Korea; the SORMA conferences in Ann Arbor and Berkeley; and an Annual Materials Research Society meeting. Additionally, one postdoctoral researcher had the opportunity to attend an advanced MCNP workshop. An MCNP module was developed for a graduate course and delivered, and a Geant4 module was redeveloped and redelivered again for the same graduate course. A graduate level lecture was also created on “Radiation backgrounds or interferences relevant to nuclear security and safeguards measurements” and delivered in a graduate level nuclear engineering course, and another lecture on “SNM characteristics” was redeveloped to include signatures from active interrogation and delivered. These modules and lectures impacted 25 additional graduate students thus far.

Three undergraduate students and a postdoctoral researcher were trained to fabricate glass samples and optically and physically characterize these samples. Six graduate students, two postdoctoral researchers, and four undergraduate students were trained in methods in a radiation instrumentation laboratory used to characterize radiation detectors with gamma and neutron sources. Moreover, two graduate students and two postdoctoral researchers were trained in methods at an accelerator facility used to characterize radiation detectors with high energy x-rays. Researchers and students were also trained in MCNP and Geant4 modeling and analysis, as described above.

### How have the results been disseminated to communities of interest?

*If there is nothing significant to report during this reporting period, state "Nothing to Report." Describe how the results have been disseminated to communities of interest. Include any outreach activities that have been undertaken to reach members of communities who are not usually aware of these research activities, for the purpose of enhancing public understanding and increasing interest in learning and careers in science, technology, and the humanities.*

Five **peer-reviewed journal papers** from work supported entirely by this project were published so far, and up to three more will be published in the coming months.

B. Ayaz-Maierhafer, X. Zhang, J.P. Hayward, Z.W. Bell, M.A. Laubach "Investigation of active background from photofission in depleted uranium using Cherenkov detectors and gamma ray time-of-flight analysis," *IEEE Transactions on Nuclear Science*, Vol. 61, No. 4, Aug. 2014, p. 2402-2409, Available: <http://dx.doi.org/10.1109/TNS.2014.2332273>

X. Zhang, J.P. Hayward, M.A. Laubach, "New method to remove the electronic noise for absolutely calibrating low gain photomultiplier tube with a higher precision," *Nuclear Instruments and Methods in Physics Research A*, Vol. 755, Aug. 2014, p. 32-37.  
Available: <http://dx.doi.org/10.1016/j.nima.2014.04.018>

B. Ayaz-Maierhafer, J.P. Hayward, Z.W. Bell, L.A. Boatner, R.E. Johnson, "Measurements of thermal neutron response in Cherenkov glass designed for MeV photon detection," *IEEE Transactions on Nuclear Science*, Vol. 60, Issue 2, May 2013, p. 701-707. Available: <http://dx.doi.org/10.1109/TNS.2013.2247420>

J.P. Hayward, Z.W. Bell, L.A. Boatner, C.L. Hobbs, R.E. Johnson, J.O. Ramey, G.E. Jellison, Jr., "Characterizing the response of Cherenkov glass detectors with isotopic gamma-ray sources," *Journal of Radioanalytical and Nuclear Chemistry*, Feb. 2013, Vol. 295, Issue 2, pp. 1143-1151. Available: <http://dx.doi.org/10.1007/s10967-012-1898-4>

J.P. Hayward, Z.W. Bell, L.A. Boatner, C.L. Hobbs, R.E. Johnson, J.O. Ramey, G.E. Jellison, Jr., "Simulated Response of Cherenkov Glass Detectors to MeV Photons," *Journal of Radioanalytical and Nuclear Chemistry*, Feb. 2013, Vol. 295, Issue 2, pp. 1321-1329. Available: <http://dx.doi.org/10.1007/s10967-012-1909-5>

The following paper is under review. Since it is not available online, a copy is included with this report.

X. Zhang, B. Ayaz-Maierhafer, M.A. Laubach, J.P. Hayward, "Observation of Material, Thickness, and Bremsstrahlung X-ray Intensity Dependent Effects in Moderate and High Z Targets in a Gamma Ray LIDAR Experiment," submitted to *Nuclear Instruments and Methods in Physics Research A*, July 2014.

The following paper is in the final stages of preparation. A two page summary of this paper is included with this report.

B. Ayaz-Maierhafer, M.A. Laubach, J.P. Hayward, "Sensing of Cf-252 Fission Gamma Rays Using Same-Size Glass Detectors," being prepared for submission to NIM A.

The following five **conference publications** also helped to disseminate this work to the scientific community:

X. Zhang, M.A. Laubach, J.P. Hayward, "Observation of material and thickness dependent effects in moderate and high Z targets in a gamma ray LIDAR experiment," SORMA, Ann Arbor, MI, June 2014.

B. Ayaz-Maierhafer, X. Zhang, M.A. Laubach, Z.W. Bell, J.P. Hayward, "Investigation of Active Background Associated with Prompt Gammas from Photofission in Depleted Uranium Using Glass Cherenkov Sensing and Gamma Ray Time-of-Flight Analysis," IEEE Nuclear Science Symposium, NP02-67, Seoul, South Korea, Oct. 2013.

J.P. Hayward, Z.W. Bell, L.A. Boatner, R. Johnson, C.L. Hobbs, J.O. Ramey, G.E. Jellison Jr., "Simulated Response of Cherenkov Glass Detectors to 6 MeV Photons," IEEE Nuclear Science Symposium in Valencia, Spain, Oct. 2011.

B. Ayaz-Maierhafter, J.P. Hayward, L.A. Boatner, Z.W. Bell, J.O. Ramey, R.E. Johnson, C.L. Hobbs, G.E. Jellison, J. Kolopus, "Phosphate Glasses for Detection of Penetrating Radiation via the Cherenkov Effect," Materials Research Society (MRS) Annual Meeting, Apr. 2011.

C.L. Hobbs, J.P. Hayward, Z.W. Bell, L.A. Boatner, J.O. Ramey, G.E. Jellison, B. Rangarajan, "Response Measurements for Cherenkov Glass Samples Using Isotopic Gamma Sources," IEEE Nuclear Science Symposium, Knoxville, TN, November 2010.

Other than peer reviewed and conference presentations, our Cherenkov glass work has also been disseminated following discussions with Rapiscan and Passport Systems, concerning fast and/or time-of-flight based active interrogation inspection; Siemens Medical Imaging, now investigating Cherenkov glasses and crystals for time-of-flight (TOF) Positron Emission Tomography (PET); Oklahoma Health Sciences Center, interested in using our glasses for improving patient care during proton therapy in radiation oncology applications; and a group of Los Alamos National Laboratory (LANL) scientists who plan to use one of our Cherenkov glasses for their measurements of subcritical fissile materials. Our work has also been shared with undergraduate nuclear engineering students, including students at UT-Knoxville and our recruiting classes, as well as with tour groups that have visited our university laboratory, e.g., UCOR (URS|CH2M Oak Ridge LLC).

# Observation of Material, Thickness, and Bremsstrahlung X-ray Intensity Dependent Effects in Moderate and High Z Targets in a Gamma Ray LIDAR Experiment

Xiaodong Zhang<sup>a,\*</sup>, Birsan Ayaz-Maierhafer<sup>a</sup>, Mitchell A. Laubach<sup>a</sup>, Jason P.  
Hayward<sup>a,b</sup>

<sup>a</sup>*Department of Nuclear Engineering, University of Tennessee, TN, USA, 37996*

<sup>b</sup>*Oak Ridge National Lab, Oak Ridge, TN, USA, 37831*

---

## Abstract

A high energy gamma ray LIDAR system consisting of a fast pulse ( $\sim 50$  ps, FWHM) LINAC and a Cherenkov detection system was used to investigate response differences among materials, their thicknesses, and bremsstrahlung X-ray intensities. The energies and pulse width of electrons used to produce bremsstrahlung X-rays were set at 20 or 40 MeV and 50 ps FWHM duration, respectively. The Cherenkov detector was built with a fused silica glass optically coupled to a 51 mm fast timing photomultiplier tube, which has an intrinsic energy threshold of 340.7 keV for Compton backscattered gammas. Such a fast detection system yields a coincidence resolving time of 93 ps FWHM, which is equivalent to a depth resolving capability of about 3 cm FWHM. The thickness of iron and lead targets were varied from one inch to seven inches with a step of one inch, and the thicknesses of DU were varied from 1/3 inch to 1 inch with a step of 1/3 inch. The experimental results show that iron targets tend to produce a factor of five less gammas, with less energetic photoelectron frequency distributions, compared with DU and lead targets for the same beam intensity and target thicknesses. Additionally, the self-shielding effect causes the lead

---

<sup>☆</sup>This material is based upon work supported by the U.S. Defense Threat Reduction Agency under Grant Award Number HDTRA 1-09-1-0052.

\*Corresponding author, email: xzhang39@utk.edu

to yield more gammas than the DU considering the experimental observation point. For the setup used in this study, a charge per pulse in the range of 1 to 2.5 nC yields a best resolving capability between the DU and lead targets.

*Keywords:* Fast Pulse LINAC, Cherenkov Detector, LIDAR

---

## 1. Introduction

Active and large-scale remote-sensing techniques widely used for in-depth probes of the atmosphere, ocean, and earth, such as microwave radars ( Radars ), optical radars ( Lidars ), and acoustical radars ( Sonars and Sodars ), are all based on the backscattering of incident interrogation beams. The reason for the prominence of a backscatter-based method is straightforward: a direct transmission-sensing system cannot be arranged in many cases. For nearly a decade, such backscattering-based remote-sensing methods have been adapted and used in a gamma remote-sensing system, commonly known as Imaging via Backscattering of Annihilation Gammas ( IBAG )[1–3]. This type of system, especially with a 3D field of view, is of particular interest for both biomedical applications and homeland security. However, limited by the small penetrating depth due to the low energy of annihilation gammas ( 511 keV ), IBAG can only be used to effectively sense moderate-scale objects. Additionally, due to the relatively low intensity of gammas from a positron emitting radioactive isotope ( e.g.,  $^{22}\text{Na}$  ) compared with that of hard Bremsstrahlung X-rays emitted from an electron linear accelerator ( LINAC ), it would take a longer time to obtain a high contrast image with a reasonable signal-to-noise ratio. This limits its application in practice.

To address these limitations, a proof-of-concept for a new backscatter-based sensing system ( See Fig. 1 ) based on a high-energy, fast-pulse LINAC and a glass Cherenkov detection system was investigated in experiments and simulations, which are discussed in detail in the following sections.

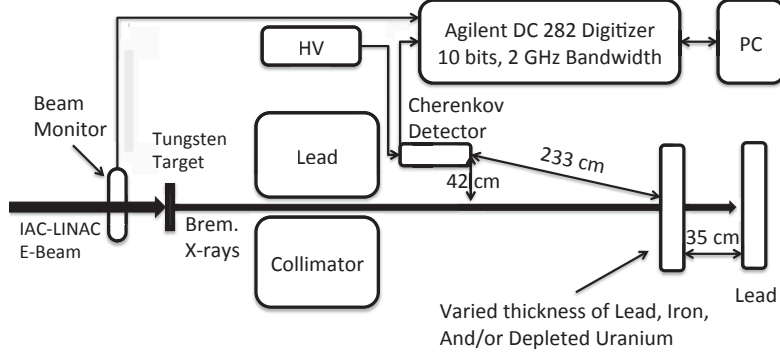


Figure 1: Experimental setup of the proposed large-scale backscatter-based sensing system with hard bremsstrahlung X-rays.

## 2. Method and Experimental Setup

In proof-of-concept experiments, the Idaho Accelerator Center ( IAC ) 44 MeV fast pulse LINAC was employed to produce high-energy bremsstrahlung X-rays. The energies and pulse width of electrons used to produce bremsstrahlung X-rays were set at 20 or 40 MeV and  $\sim 50$  ps FWHM duration, respectively. The pulse repetition rate was 120 Hz. A fast-timing, high efficiency glass Cherenkov detection system [4–6] was used to detect the backscattered X-rays and secondary gamma rays. The different contributors to the observed gamma and x-ray signals were explained in [6]. The Cherenkov detector reported here was built with a fused silica glass optically coupled with a 51 mm Hamamatsu H10570 photomultiplier tube assembly. As shown in Fig. 1, the detector was mounted at 42 cm off the beam axis and 233 cm away from the first target layer. From this setup, if scaling up to a square meter size detector is considered for standoff detection, air attenuation aside, the solid angle coverage used here for one detector is equivalent to a standoff distance of 65.7 m [6]. An Agilent DC 282 digitizer with 10 bit resolution and 2 GHz bandwidth was used to directly record the pulses from the Cherenkov detector and the IAC beam monitor with a sampling rate of 4 GSa/s. The digitized waveform was integrated in order to determine the charge of the pulse, recorded as the number of photoelectrons.



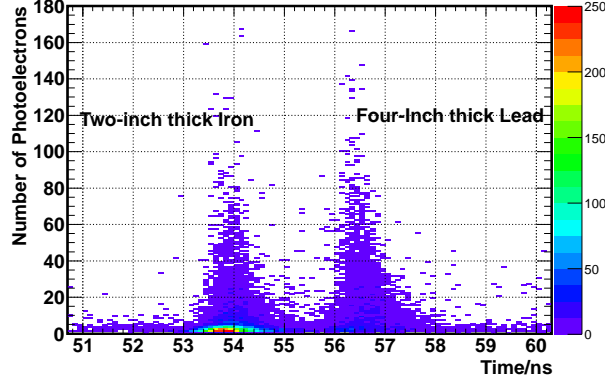


Figure 2: Histogram of photoelectrons vs. pickoff time of detector signals from a two-inch thick iron target separated from a four-inch thick lead target.

43 This system has a coincidence resolving time of 93 ps FWHM[6]. Such a good  
 44 system timing resolution yields a depth resolution of  $\sim 3$  cm FWHM. This reso-  
 45 lution is good enough for scanning many medium to large scale objects, such as  
 46 cargo containers, small vessels, and shallow buried underground moderate and  
 47 high-Z objects.

48 With the system depicted in Fig.1, three different configurations of targets  
 49 consisting of a combination of varied thicknesses of iron or lead or depleted ura-  
 50 nium (DU) in front of a four-inch lead brick were studied (or a two-inch lead  
 51 brick for the lead target). These lead bricks were placed in front of a transmis-  
 52 sion detector (results not shown) in order to establish the proper dynamic range  
 53 for it. The thicknesses of iron and lead were varied from one inch to seven inches  
 54 with a step of one inch, and the thicknesses of DU were varied from 1/3 inch to  
 55 1 inch with a step of 1/3 inch. The distance between the target objects in the  
 56 targets was set as 35 cm in experiments, resulting in a back-and-forth gamma  
 57 travel time of 2.33 ns.

### 3. Results and Discussion

#### 3.1. Depth Resolving Capability

The number of photoelectrons plotted against the time of the signals from the target composed of two-inch iron in front of the four-inch lead is shown in Fig. 2, as an example. Here, a digital constant fraction discriminator with a constant fraction of 0.2 was proved to be the best for precisely picking off the time for each signal in the data analysis. Fig. 2 clearly shows that the interactions corresponding to higher energy deposition, and therefore tending toward larger photoelectron numbers show clearer separation between the iron and lead layers compared with the interactions corresponding to lower energy deposition, e.g., at 10 photoelectrons and below. Said another way, when looking only at higher photoelectron numbers, the estimate of the distance between the lead and iron targets, corresponding to 2.33 ns in time separation, is more accurate. A quantitative analysis of Fig. 2 shows that the separation in time between two responses changes from  $2.21 \pm 0.42$  ns at a threshold of one photoelectron to an almost constant value of  $2.31 \pm 0.26$  ns at and above a threshold of 15 photoelectrons. The poor estimate of depth when all the data is used is mainly caused by the long lifetime of positrons produced through the annihilation process in bulk materials, corresponding to about 110 ps in iron and 194 ps in lead[7]. Referring to Fig. 2, this difference in lifetimes causes the base of the distribution corresponding to the lead target to be wider than that of the distribution corresponding to the iron target. This statement is supported in that the absolute calibration of the Cherenkov detector shows that the peak, or most probable, response for 511-keV gammas is one[8].

#### 3.2. Responses of Different Targets and Thicknesses

The detector response to iron, lead, and DU of various thicknesses was investigated experimentally using 20 MeV bremsstrahlung X-rays. The integrated signal charge was normalized to the integrated charge of a 5.0 nC electron pulse, as shown in Figures 3 and 4. One can see from Figure 3 as an example that

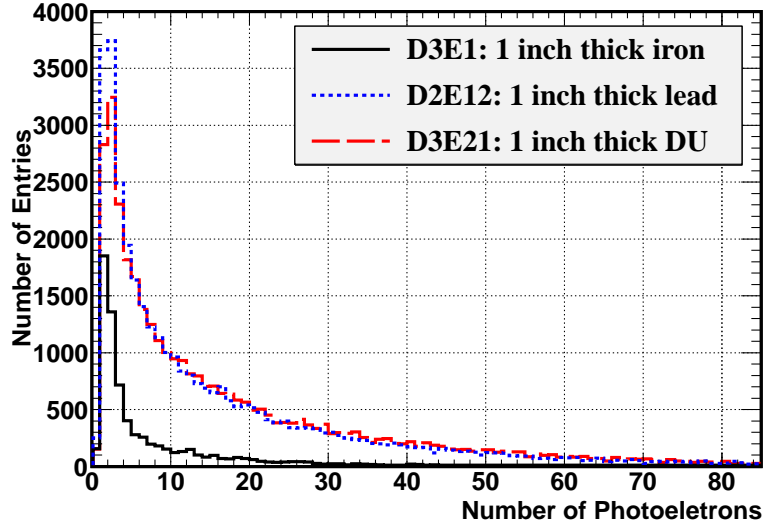


Figure 3: Distributions of the integrated charge from signals from one-inch thickness of iron, lead, or DU targets.

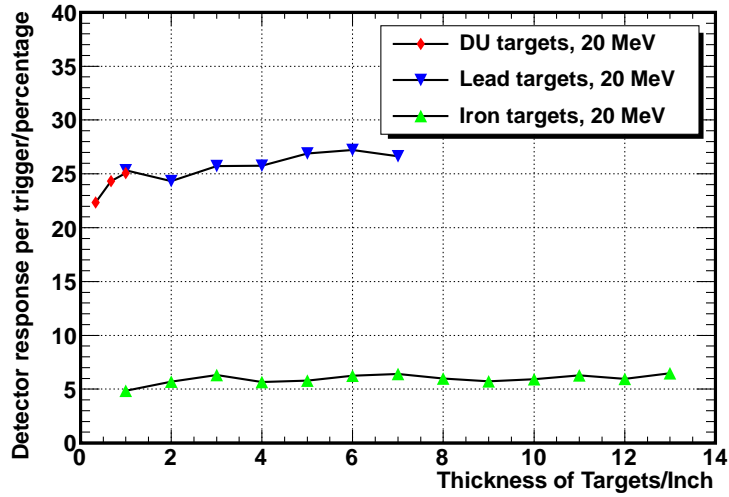


Figure 4: Detector response to different thicknesses of iron, lead, and DU with 20 MeV bremsstrahlung X-rays.

87 one-inch thick lead and DU targets produce more gammas and these photo-  
 88 electron frequency distributions are harder compared with that from the iron  
 89 target. This was also found to be true for other thicknesses of the same ma-  
 90 terials (data not shown). In Figure 4, the possibility of detecting at least one  
 91 gamma (displayed as percentage response) from each 5.0 nC pulse is shown for  
 92 the various target materials and thicknesses. Additionally, one can also see from  
 93 Figures 3 and 4 that for one-inch targets, lead tends to produce more gammas  
 94 compared with the same thick DU target. To understand the reason, Monte  
 95 Carlo-N Particle (MCNPX) simulation kit[9] was used to model the experi-  
 96 mental setup based upon our experimental geometries and parameters. In the  
 97 MCNPX simulation, we tallied the gamma rays crossing the opposite direc-  
 98 tion (backwards) of the surface (where the incident gammas enter) for various  
 99 lead and DU thicknesses. Figure 5 shows the tally result as a function of target  
 100 thicknesses at 20 and 40 MeV. From the simulation results, one sees that once  
 101 the thickness of target is larger than 15 mm for 20 MeV and 20 mm for 40 MeV,

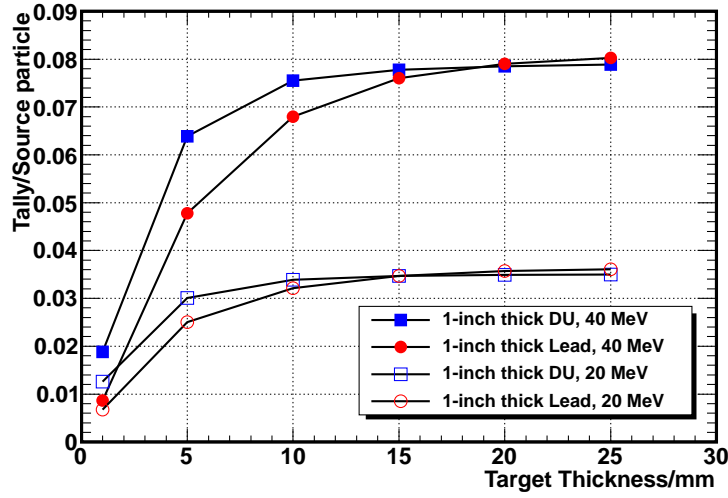


Figure 5: Expected gamma yields from different thick lead and DU targets for bremsstrahlung X-rays at 20 and 40 MeV.

102 gamma yields for lead targets become larger than DU targets. This can be  
 103 explained as the familiar self-shielding effect. Specifically, DU has higher cross  
 104 sections for the Compton scatter, annihilation, and secondary bremsstrahlung  
 105 processes compared with lead. But this applies to photons going both ways,  
 106 i.e., the larger cross sections cause the DU targets to produce more gammas at  
 107 a backward angle, but when these gammas pass back through the same target,  
 108 the larger cross sections also act with higher stopping power to absorb them or  
 109 scatter them away from the detector. So when the thickness reaches some par-  
 110 ticular value, the later absorbing and scattering reactions will dominate, causing  
 111 a smaller observed gamma rate.

112 Additionally, both Figures 3 and 4 show a clear separation between iron  
 113 (medium Z) targets and lead/DU (high Z) targets at the same thicknesses,  
 114 which can be explained below. Since the Cherenkov detector used in the ex-  
 115 periment has an intrinsic energy threshold of 340.7 keV (Compton scatter), the  
 116 Compton scattering gammas at the observation point are unlikely to be regis-  
 117 tered. In contrast, the annihilation and secondary bremsstrahlung gammas can  
 118 be recorded due to their higher energies. These phenomena happen to facilitate  
 119 our ability to resolve material Z since Compton scattering (unlikely to be regis-  
 120 tered) depends on Z while annihilation and secondary bremsstrahlung have  $Z^2$   
 121 or higher order dependencies.

### 122 *3.3. Response for Different X-ray Intensities*

123 Experimental results of detector response to one-inch thick lead or DU tar-  
 124 gets as a function of different charge per pulse at 40 MeV are shown in Figure 6.  
 125 One can see that the lead targets tend to produce more gammas at back an-  
 126 gles compared with the DU targets. In order to achieve good separation in the  
 127 response between lead and DU, the charge per pulse should be chosen in the  
 128 range of 1 to 2.5 nC. Neither too large or too small is good to better resolve the  
 129 DU and lead targets. Larger charge of electron pulse means a larger amount  
 130 of bremsstrahlung X-rays per pulse, which also means more gamma yield. But  
 131 once the charge of pulse is larger than 2.5 nC, the gamma yields tend to get to a

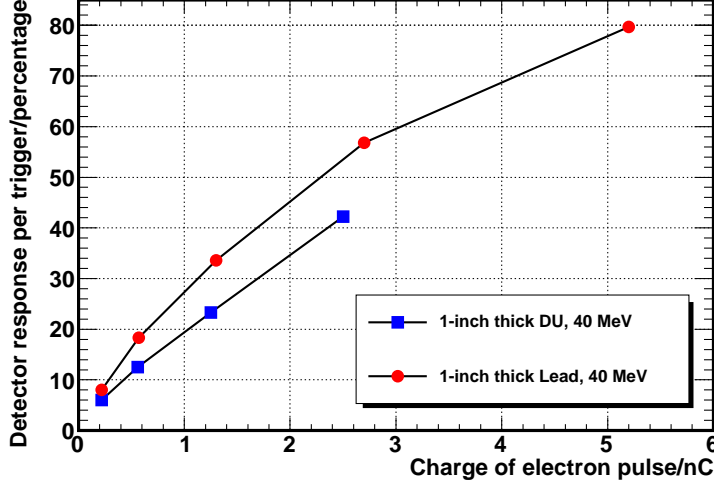


Figure 6: Detector response to one-inch thick lead and DU layers for different charges of electron pulses used to produce bremsstrahlung X-rays at 40 MeV.

132 saturation point, which can be explained that higher intensity of bremsstrahlung  
 133 X-rays will increase the possibility of two or more gammas are detected by the  
 134 detector. Referring back to Figure 6, smaller charge per pulse means lower in-  
 135 tensity of bremsstrahlung X-rays, leading to lower detection statistics, and thus,  
 136 a degraded ability to tell DU from lead using the 40 MeV beam.

#### 137 4. Summary

138 In summary, the response of a gamma ray LIDAR system to different mod-  
 139 erate and high Z target materials and thicknesses was investigated. The sys-  
 140 tem consisted of a fast pulse ( $\sim 50$  ps) LINAC and a Cherenkov detector. The  
 141 sub-100 ps timing resolution allows the system to achieve 3 cm depth resolving  
 142 ability. The long lifetime of positrons produced through the annihilation pro-  
 143 cess in targets, such as 110 ps in iron and 194 ps in lead, will worse the depth  
 144 resolving ability of the detection system. Thus, a higher threshold is desirable to  
 145 mitigate this influence. Because the intrinsic energy threshold of the Cherenkov

146 detector is 340.7 keV, Compton scattering gammas in the experimental refer-  
 147 ence frame are not registered by the detector due to their low energies. Thus,  
 148 only annihilation and high energy secondary bremsstrahlung gammas with a  
 149  $Z^2$  or higher order dependence are recorded by the detector, which increases  
 150 the system material or Z resolving capability compared with detection systems  
 151 which are sensitive to Compton scattering gammas depended on Z. Taking this  
 152 advantage, a factor of five of gamma yield difference between iron targets and  
 153 DU/lead targets have been observed for bremsstrahlung X-ray at 20 MeV. In  
 154 addition, referring to Figure 3, experiments show that iron targets tend to pro-  
 155 duce less energetic gammas compared with lead and DU targets. Combining  
 156 this with gamma yields of targets, a better material resolving capability should  
 157 be obtained.

158 Furthermore, due to the self-shielding effect, simulations with a MCNPX  
 159 model show that lead targets produce more gammas than DU targets when  
 160 the target thicknesses are larger than 15 mm and 20 mm for bremsstrahlung X-  
 161 rays at 20 and 40 MeV, respectively. Experimental results for one-inch thick  
 162 lead and DU target at 20 MeV show consistency with simulation results. The  
 163 experimental results with various charge per pulse for bremsstrahlung X-rays at  
 164 40 MeV also suggest that using the charge per pulse in the range of 1 to 2.5 nC  
 165 can yield a better separation between lead and DU targets in the same situations  
 166 with our setup. Thus, in a given system, an optimized bremsstrahlung X-ray  
 167 intensity is necessary to achieve a best resolving capability of materials or Zs.

168 In conclusion, in term of best material or Z resolving capability, a suitable  
 169 energy threshold of Cherenkov detectors and an optimal bremsstrahlung X-ray  
 170 intensity are important.

## 171 References

- 172 [1] L. Gurdev, D. V. Stoyanov, T. Dreischuh, C. Protochristov, O. Vankov,  
 173 Gamma-Ray Backscattering Tomography Approach Based on the Lidar  
 174 Principle, Nuclear Science, IEEE Transactions on 54 (1) (2007) 262–275.

- [2] Q. Looker, L. Stonehill, M. Wallace, M. Galassi, M. Cowee, E. Fenimore,  
W. V. McNeil, Demonstration of imaging via backscattering of annihilation  
gamma rays, Nucl. Instr. and Meth. A 615 (3) (2010) 295 – 300.
- [3] C. Domingo-Pardo, A new technique for 3d gamma-ray imaging: Conceptual  
study of a 3d camera, Nucl. Instr. and Meth. A 675 (0) (2012) 123 – 132.
- [4] J. P. Hayward, C. L. Hobbs, Z. W. Bell, L. A. Boatner, R. E. Johnson, J. O.  
Ramey, G. E. Jellison, Characterizing the radiation response of Cherenkov  
glass detectors with isotopic sources, J. Radioanal. Nucl. Chem. 295 (2)  
(2013) 1143–1151.
- [5] J. P. Hayward, Z. W. Bell, L. A. Boatner, C. L. Hobbs, R. E. Johnson, J. O.  
Ramey, G. E. Jellison, Simulated response of Cherenkov glass detectors to  
Mev photons, J. Radioanal. Nucl. Chem. 295 (2) (2013) 1321–1329.
- [6] B. Ayaz-Maierhafer, X. Zhang, J. P. Hayward, Z. W. Bell, M. A. Laubach,  
Investigation of active background from photofission in depleted uranium  
using Cherenkov detectors and gamma ray time-of-flight analysis, Accepted  
by Nuclear Science, IEEE Transactions on, Jun. 18, 2014.
- [7] B. Barbiellini, P. Genoud, T. Jarlborg, Calculation of positron lifetimes in  
bulk materials, J. Phys.: Condens. Matter 3 (1991) 7631–7640.
- [8] X. Zhang, J. P. Hayward, M. A. Laubach, New method to remove the elec-  
tronic noise for absolutely calibrating low gain photomultiplier tubes with a  
higher precision, Nucl. Instr. and Meth. A 755 (2014) 32–37.
- [9] F. Brown, J. Bull, J. Goorley, A. Sood, J. Sweezy, MCNP5-1.51, LA-UR-  
09-00384.



# Sensing of Cf-252 fission gamma rays using same size glass Cherenkov detectors

B.Ayaz-Maierhafer<sup>1</sup>, J.P. Hayward<sup>1,2</sup>, M.A.Laubach<sup>1</sup>

<sup>1</sup>*The University of Tennessee, Knoxville, TN, United States*

<sup>2</sup>*Oak Ridge National Laboratory, Oak Ridge, TN, United States*

CHERENKOV detectors have been investigated in many radiation detection applications including neutron and gamma ray sensing [1 - 5]. Response to the interaction of typical low energy neutron or isotopic gamma sources yields from one to tens of photoelectrons in a photomultiplier tube. In a previous study, we demonstrated that glass Cherenkov detectors are able to sense induced fission gamma rays when a depleted uranium target was bombarded with MeV x-rays produced by a Short Pulse Linear Accelerator [6]. Furthermore, we found that it sensed prompt active gamma background with greater frequency than prompt fission gammas from photofission.

When it comes to fission gamma ray sensing, it is not clear how the detection efficiency of glass detectors depends on particular properties of the glass such as its density and optical absorption edge. That is the subject of this work. Since Cherenkov detectors do not produce much light when gammas or neutrons interact (order of tens to hundreds of optical photons), light production and collection affects the observed detection efficiency.

Specifically, the objective of this experimental work was to investigate the capabilities of glass Cherenkov detectors to sense <sup>252</sup>Cf fission gammas and neutrons through time-of-flight (TOF) analysis. <sup>252</sup>Cf decays 96.91% of the time by alpha emission; spontaneous fission (SF) is the alternative decay mode in the remaining 3.09% of decay events. The spontaneous fission process leads to the prompt emission of fission neutrons and gamma rays. The prompt gamma rays from SF of <sup>252</sup>Cf are, on average, 0.87 MeV, with ~8 emitted per fission [7].

Eight same-size Cherenkov detectors were tested, including 7 glasses and one crystal, all of which were purchased from commercial sources. They were chosen to vary in density, refractive index and optical absorption. One large glass detector fabricated by Oak Ridge National Laboratory (ORNL) and discussed in [3-5] was also included in the same set. The physical dimensions, density, refractive index ( $n$ ), the fraction of the gammas stopped, the Cherenkov gamma threshold energy ( $E_{th\_gamma}$ ) and the optical absorption edge of the detectors are listed in Table I. The fraction of gammas stopped is calculated for the mean fission gamma energy using the total cross section. The intrinsic threshold is simply a function of the refractive index. The glass Cherenkov detectors include a fused silica glass (Corning 7980 ARF) and materials N-AF34, SF-57, N-LAK22, N-LAF7, N-SF11, N-SK5 (Schott catalog info given, compositions are proprietary). The ORNL glass is Magnesium Cesium Phosphate (abbreviated MgCs Phosphate), as described in [5]. The only crystal used was PbF<sub>2</sub>, a well known Cherenkov radiator. It was used become glasses so dense and transmissive are

difficult to come by. The crystal used is the same size as the 7 glasses after polishing. For uniformity, all Cherenkov detectors were polished on both top and bottom but not the sides.

The experimental setup consisted of a <sup>252</sup>Cf ionization chamber irradiating a Cherenkov detector made from a Hamamatsu R2059 PMT with quartz window optically coupled to the glass. The glasses were wrapped in Teflon tape. The ion chamber serves to time tag the fission events. An electronic threshold was set to discriminate between alpha pulses and fission fragment pulses. An Aquiris DC282 digitizing system was set to collect data in the case of coincidence between the ionization chamber and the Cherenkov detector. The distance between the detector and the source was 27 cm. Since the time of flights for gammas and neutrons (endpoint energy for watt spectrum ~ 6 MeV) are 30 cm/ns and 3.4 cm/ns, respectively, this distance gives a clear separation between the gamma and neutrons through TOF analysis.

The digitized waveforms from the Cherenkov glass detectors were post processed to determine their integrated charge. Integrated charge distributions are a measure of the light produced and also of the deposited energy from gamma interactions. Fig. 1a shows the time-of-flight frequency distribution, and Fig. 1b shows the combined time-of-flight and integrated charge image (for 10,000 waveforms) for one of the glasses that had been tested. As seen from Fig. 1a, the response from the gamma rays is located in the first part of the TOF distribution (~15 ns), and the later arriving particles (after 20 ns) are either from scattered gamma rays from the walls or from inelastic neutron scattering in the glass detector. The count rates from direct fission gamma rays and neutrons/scattered gammas for each glass are given in Table I. The count rates from direct fission gamma ray sensing are 13-20 times higher than the count rates from the neutrons/scattered gammas.

Referring to Table I, the highest and the lowest count rates were obtained for PbF<sub>2</sub> and N-SF11, respectively. For same size detectors with surfaces treated identically, the absorption edge and the density both clearly have a significant impact on the fission gamma count rate. While the density dependence is largely intuitive<sup>1</sup>, the observed count rate dependence on optical absorption edge is particularly remarkable. For example, if we compare the N-LAF7 and N-LAK22 detector response, these two glasses have very similar densities (3.73 g/cm<sup>3</sup> and 3.77 g/cm<sup>3</sup>), yet the count rate is two times of higher for N\_LAK22 (1.03 cps) compared with

<sup>1</sup> Higher density means greater interaction probability. This clearly dominates over the effect of shorter electron/positron track length until  $E_h$  is reached, resulting in less light production compared with less dense detectors.

N\_LAF7 (0.5 cps). This is the case even though N\_LAK22 has higher threshold energy (260 keV) than N-LAF7 (233 keV), so it should produce less total Cherenkov light. Yet, the lower optical absorption edge of N-LAK22 compared with N-LAF7 (326 nm versus 379 nm, respectively) results in much greater transmission of the more abundant ( $\propto 1/\lambda^2$ ) low wavelength ( $\lambda$ ) Cherenkov photons. Consider that some minimum number of photoelectrons (e.g., 2) must be registered by the system to yield a count. This low absorption edge is clearly the reason that the fission gamma count rate is so much higher for the N-LAF7 glass detector compared with the N-LAK22 glass detector.

Another data point that shows the importance of the optical absorption edge is that from fused silica. The fused silica glass has the lowest density (2.2 g/cm<sup>3</sup>) and the highest threshold energy (341 keV) of any detector in this study. Yet, since the absorption edge is very low (190 nm), the count rate is higher than all of the following more dense glasses which have higher absorption edges: N-SF11, NSK-5, N-LAF7, N-LAF34, SF-57. In fact, the only glass detector in this set with a higher count rate than fused silica is N-LAK22, which has a density of 3.77 g/cm<sup>3</sup> and a low absorption edge of 326 nm.

TABLE I  
PROPERTIES AND THE COUNT RATES OF THE GLASS SAMPLES

Glass Sample	Diameter/ Thickness (mm)	Density (g/cm <sup>3</sup> )	$n$ (600 nm)	Absorption edge (nm)	$E_{th, \gamma}$ (keV)	Fraction of $\gamma$ 's stopped (for 0.87 MeV)	Count rate from gamma ray sensing (cps)	Count rate from neutron /scattered gamma ray sensing (cps)
Fused silica	51/36	2.20	1.45	190	341	0.42	0.94±1.17E-4	0.036±9.14E-5
MgCs Phosphate	55/30	3.15	1.54	240	299	-	0.47±5.1E-5	0.026±4.66E-5
N-SF11	51/36	3.22	1.78	383	227	0.55	0.38±4.19E-5	0.0212±3.81E-5
N-SK5	51/36	3.30	1.59	315	280	0.56	0.90±1.17E-4	0.045±8.96E-5
N-LAF7	51/36	3.73	1.75	379	234	0.60	0.50±1.01E-4	0.038±5.04E-5
N-LAK22	51/36	3.77	1.65	326	260	0.60	1.03±1.37E-4	0.058±1.02E-4
N-LAF34	51/36	4.24	1.77	325	229	0.65	0.82±1.06E-4	0.047±8.16E-5
SF-57	51/36	5.51	1.85	379	212	0.74	0.62±8.76E-5	0.033±6.23E-5
PbF <sub>2</sub>	51/36	7.77	1.82	290	218	0.89	1.65±2.03E-4	0.127±1.65E-4

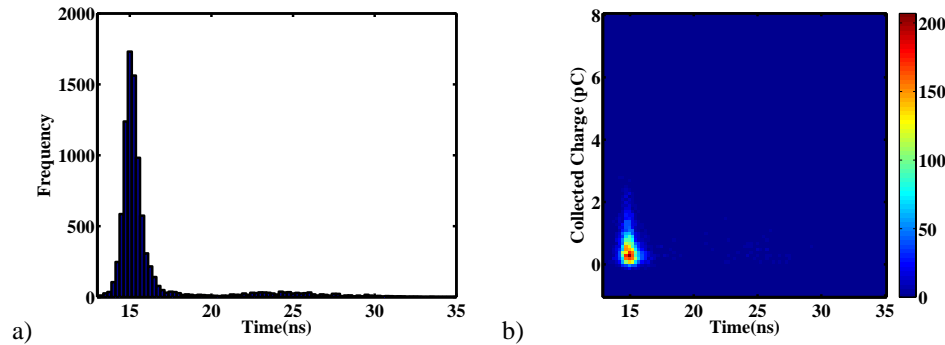


Fig. 1. a) The time-of-flight frequency distribution, and b) the combined time of flight and collected charge image for PbF<sub>2</sub>

Referring to Table I, if we compare two same-size Cherenkov detector that have similar absorption edges and threshold energies, for example N-SF11 (absorption edge =383 nm, threshold energy =227 keV) and SF-57 (absorption edge =379 nm, threshold energy =212 keV), the fission gamma count rate is higher for SF-57 (0.62 cps) compared to N-SF11 (0.38 cps) because SF-57 has much higher density. Clearly, this increase count rate is due to a higher total cross section, resulting in a higher probability of stopped gamma rays. At 0.87 MeV, the chance of a gamma ray stopping in the SF-57 is 26% higher.

Cherenkov detectors for fission gamma sensing should be dense and have a low optical absorption edge. This is consistent with what has been observed for Cherenkov radiators used in high energy physics to sense various types of electromagnetic radiation.

#### REFERENCES

- [1] S. Dazeley, A. Bernstein, N.S. Bowden, R. Svoboda, *Nucl. Instr. And Meth. A*, vol. 607, pp. 616-619, 2009.
- [2] Z.W. Bell, L.A. Boatner, "Neutron detection via the Cherenkov effect," *IEEE Trans. Nuc. Sci.*, vol. 57, pp. 3800-3806, 2010.
- [3] B. Ayaz-Maierhafer, J.P. Hayward, Z.W. Bell, L.A. Boatner, and R.E. Johnson, *IEEE Trans. Nucl. Sci.*, vol. 60, pp. 701-707, 2013.
- [4] J.P. Hayward et al, *J. Radioanal. Nucl. Ch.*, vol. 295, pp.1143-1151, 2013.
- [5] J.P. Hayward et al, *J. Radioanal. Nucl. Ch.*, vol. 295, pp. 1321-1329, 2013.
- [6] B. Ayaz-Maierhafer, X. Zhang, J.P. Hayward, Z.W. Bell, M.A. Laubach, " *IEEE Trans. Nucl. Sci.* , under review.
- [7] Radiation Shielding, J. K. Shulitis and R.E.Faw.ISBN-10: 0894484567

**DISTRIBUTION LIST  
DTRA-TR-15-9**

**DEPARTMENT OF DEFENSE**

DEFENSE THREAT REDUCTION  
AGENCY  
8725 JOHN J. KINGMAN ROAD  
STOP 6201  
FORT BELVOIR, VA 22060  
ATTN: D. PETERSEN

DEFENSE THREAT REDUCTION  
AGENCY  
8725 JOHN J. KINGMAN ROAD  
STOP 6201  
FORT BELVOIR, VA 22060  
ATTN: G. DOYLE

DEFENSE TECHNICAL  
INFORMATION CENTER  
8725 JOHN J. KINGMAN ROAD,  
SUITE 0944  
FT. BELVOIR, VA 22060-6201  
ATTN: DTIC/OCA

**DEPARTMENT OF DEFENSE  
CONTRACTORS**

QUANTERION SOLUTIONS, INC.  
1680 TEXAS STREET, SE  
KIRTLAND AFB, NM 87117-5669  
ATTN: DTRIAC